Surfactant Protein SP-B Strongly Modifies Surface Collapse of Phospholipid Vesicles: Insights from a Quartz Crystal Microbalance with Dissipation

Elisa J. Cabré,[†] Jenny Malmström,[‡] Duncan Sutherland,[‡] J. Pérez-Gil,[†*] and Daniel E. Otzen[‡*]
[†]Departamento Bioquímica y Biología Molecular I, Facultad de Biología, Universidad Complutense, Madrid, Spain; and and [‡]Interdisciplinary Nanoscience Research Center and Department of Molecular Biology, University of Aarhus, Aarhus, Denmark

ABSTRACT Pulmonary surfactant protein B (SP-B) facilitates the rapid transfer of phospholipids from bilayer stores into air-liquid interfacial films along the breathing cycle, and contributes to the formation of a surface-associated multilayer reservoir of surfactant to optimize the stability of the respiratory interface. To obtain more insights into the mechanisms underlying this transfer and multilayer formation, we established a simple model system that captures different features of SP-B action. We monitored the formation of supported planar bilayers from the collapse of intact phospholipid vesicles on a silica surface using a technique called quartz crystal microbalance with dissipation, which provides information on changes in membrane thickness and viscosity. At physiologically relevant concentrations, SP-B dramatically alters vesicle collapse. This manifests itself as a reduced buildup of intact vesicles on the surface before collapse, and allows the stepwise buildup of multilayered deposits. Accumulation of lipids in these multilayer deposits requires the presence of SP-B in both the receptor and the arriving membranes, surrounded by a comparable phospholipid charge. Thus, the quartz crystal microbalance with dissipation system provides a useful, simplified way to mimic the effect of surfactant protein on vesicle dynamics and permits a detailed characterization of the parameters governing reorganization of surfactant layers.

INTRODUCTION

Lung surfactant (LS) is composed of roughly 90% lipids and 8–10% of a few specific surfactant-associated proteins, termed in chronological order of discovery SP-A, SP-B, SP-C, and SP-D. The most abundant phospholipid species in LS is dipalmitoylphosphatidylcholine (DPPC), which is also the main surface-active component (1). However, it has become clear after many years of biophysical studies that these surfactant lipids are unable to segregate unaided to the air-liquid interface at a sufficiently rapid rate, once they are secreted by type II pneumocytes, to form operative surface-active films that are able to stabilize the respiratory interface during successive compression-expansion cycles. The presence of hydrophobic surfactant proteins SP-B and SP-C is strictly required to facilitate an efficient transfer of phospholipids from LS stores (in the form of bilayers) into the interfacial film through the aqueous hypophase (2,3). Most therapeutic surfactant preparations currently in use are obtained from animal sources and contain variable amounts of SP-B and SP-C (4). However, the molecular mechanisms by which surfactant proteins participate in the assembly, transport, and reorganization of surfactant lipids at the respiratory surface are still not well understood.

SP-B is essential from the very first inspiration at birth (5). In humans, a lack of SP-B causes lethal respiratory failure similar to that observed in SP-B-deficient genetically modified mice (6–8). Absence of SP-B is accompanied by an incomplete processing of the SP-C precursor (9,10). SP-B is also strictly required for the biogenesis and packing of pulmonary surfactant into lamellar bodies (11,12). The essential role of SP-B has been related to the ability of the protein to promote a rapid transfer of phospholipids into air-water interfaces to establish an operative surface-active film from the earliest formed respiratory interface. The protein has been suggested to interact peripherally with phospholipid membranes, with the main axis of some amphipathic helices orientated parallel to the plane of the lipid layers (13–15). SP-B has been reported to promote more or less deep perturbations in membranes leading to lipid exchange and eventual fusion between liposome membranes and rapid leakage of their content (16–18). Destabilization of lipid packing could be part of the mechanism by which SP-B initiates exchange of phospholipids between LS membranes and the interfacial film. Indeed, it has been proposed that hydrophobic surfactant proteins stabilize transition intermediates in interfacial adsorption (19). A cluster of aromatic residues near the N-terminus defines the high affinity of SP-B to interact with interfacial regions of phospholipid layers (20). This affinity is crucial for inserting LS rapidly enough into the interface during the brief periods of expansion at inspiration (21).

The proposed central role of SP-B in phospholipid vesicle dynamics makes it important to study SP-B-modulated surfactant vesicle properties in as many complementary ways as possible. In this study we used a surface-layer technique called quartz crystal microbalance with dissipation (QCM-D) to obtain information on how SP-B affects the collapse and reorganization of phospholipids on surfaces.

Submitted February 28, 2009, and accepted for publication April 29, 2009.

*Correspondence: dao@inano.dk or jpg@bbm1.ucm.es

Editor: William C. Wimley.

0006-3495/09/08/0768/9 $2.00

doi: 10.1016/j.bpj.2009.04.057

QCM-D measures changes in the crystal resonance frequency and the dissipation of oscillations. The frequency change is related to the amount of deposited mass, but this relationship is affected by the degree of coupling between the film and the underlying surface, which in turn is expressed through the dissipation (22,23). Together, these two parameters can be interpreted within the framework of the Voight viscoelastic model for deposition of films at solid-liquid interfaces to obtain information on changes in membrane thickness and viscosity (24). Thus, QCM-D allows us to follow the different steps associated with vesicle colonization of a surface, the collapse of these vesicles to form supported bilayers, and the formation of additional layers on top. We show that the presence of SP-B profoundly affects the different collapse steps and facilitates the buildup of multilayer deposits. Thus, surface collapse of surfactant-containing vesicles on a silica surface monitored by QCM-D may provide a useful model system for elucidating more details of the molecular mechanisms associated with LS function.

MATERIALS AND METHODS

Materials

The lipids 1,2-dioleyl-s*n*-glycero-3-phosphocholine (DOPC), 1-palmitoyl-2-oleoyl-*sn*-glycero-3-phosphocholine (POPC), 1-palmitoyl-2-oleoyl-*sn*-glycero-3-[phospho-*rac*-(1-glycerol)] (POPG), and 1,2-dipalmitoyl-s*n*-glycero-3-phosphocholine (DPPC) were from Avanti Polar Lipids (Alabaster, AL). Chloroform and methanol (HPLC grade), NaCl, HEPES (2-[4-(2-hydroxyethyl)-1-piperazinyl]ethanesulfonic acid), and $CaCl_2$ were obtained from Merck A/S (Darmstadt, Germany). Buffers were prepared with MQ water (MilliQ A10; Millipore, Zug, Switzerland), filtered through a 0.2 μm pore filter and degassed by sonication before use. The buffers used were 50 mM HEPES, pH 7, containing 150 mM NaCl and $CaCl_2$ 2 mM when needed. Surfactant protein SP-B was isolated from minced porcine lungs as described previously (25) by two consecutive chromatographic steps in Sephadex LH-20 and LH-60 gels (Pharmacia, Uppsala, Sweden). The protein was routinely checked for purity by sodium dodecyl sulfate polyacrylamide gel electrophoresis, and quantified by amino acid analysis. Electrophoretic and mass spectrometry analysis of purified SP-B fractions revealed that >90% of the protein consists of covalent dimers. Isolated SP-B was stored in chloroform/methanol 2:1 (v/v) solutions at −20°C until used. Polymyxin B sulfate (Aerosporin, PMB) was purchased from Fluka (St. Louis, MO), dissolved in methanol at 0.1 mg/mL, and stored at −20°C until used.

Preparation of large unilamellar vesicles

The different phospholipids (typically 1 mg) used in these experiments were dissolved in chloroform in a round-bottomed flask. To ensure that we always retained phospholipids in the liquid disordered state, most experiments were carried out using unsaturated phospholipids (DOPC and DOPG) with melting temperatures well below 0°C.

Whenever used, SP-B was mixed with lipids in chloroform and dried together. The chloroform was evaporated using a flow of N_2 gas to form a thin, dried lipid film on the wall of the flask. Buffer (see next section) was added to the dry lipid film to achieve a lipid concentration of 1 mg/mL. To form large unilamellar vesicles (LUVs) with a nominal diameter of 100 nm, the extrusion method was applied by passing the solution back and forth 11 times through a polycarbonate membrane with a matching pore size in a mini-extruder from Avanti Polar lipids. Each extruded milliliter was diluted 10 times to obtain a final concentration of 0.1 mg/mL of lipid in every experiment.

QCM-D experiments

A Q-sense E-4 quartz microbalance device and silica (silicon dioxide)-coated AT-cut quartz crystals with a fundamental resonance frequency of ~5 MHz and bare gold electrodes were purchased from Q-Sense AB (Gothenburg, Sweden). The data were collected in Q-Soft 401 and analyzed in Q-Tools. All experiments were performed at 25°C in 150 mM NaCl, 1 and 50 mM HEPES, pH 7, with a continuous flow of 0.1 mL/min; 2 mM $CaCl_2$ were included in all experiments involving anionic lipids to avoid repulsion of negatively charged membranes and facilitate collapse. Calcium had no effect on the experiments with zwitterionic lipids, which are only shown in the absence of the cation. The silica crystals were cleaned using a cleaning holder (QClH 301, Q-sense AB, Gothenburg, Sweden), 10% sodium dodecyl sulfate, and 15 W UV oven as described previously (26). Each experiment was performed at least three times to ensure reproducibility. The concentration of vesicles was 0.1 mg/mL and the proportion of SP-B in the membranes ranged from 0.1% to 4% (w/w). All frequency values Δf recorded at different overtones n and mentioned in the text are normalized with the factor $1/n$ to allow direct comparison.

RESULTS

Adsorption and collapse of zwitterionic LUVs

Fig. 1 *a* shows typical QCM-D profiles of the frequency and dissipation changes that occur during the spontaneous collapse of DOPC vesicles (LUVs) over the silica surface to form a supported planar lipid bilayer. In the first step after introduction of the vesicles into the chamber, the vesicles begin adsorbing on the silica surface and the oscillation frequency decreases (as a consequence of the increase in

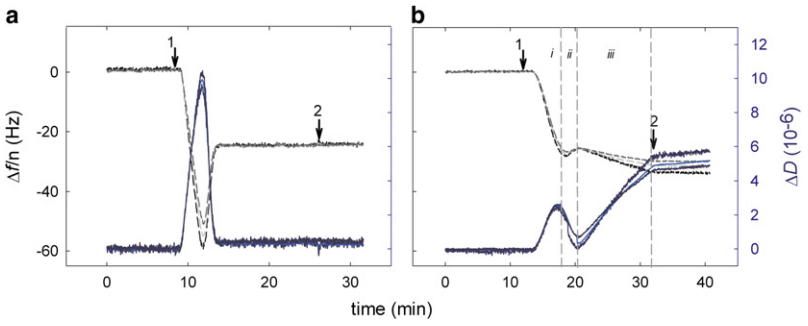

FIGURE 1 Frequency shift and dissipation profiles of DOPC and DOPC/SP-B vesicles adsorbed onto a silica surface. Typical QCM-D profiles of frequency (*black*) and dissipation (*blue*) changes upon adsorption of DOPC LUVs (0.1 mg/mL), in the absence (*a*) or presence (*b*) of SP-B 1% (protein to lipid, w/w), onto a silica surface pre-equilibrated with buffer HEPES 50 mM, pH 7, containing NaCl 150 mM. Data from overtones 5, 7, and 9 are plotted in different color tones. At point 1, lipid or lipid/protein vesicles were injected after a stable baseline was obtained in buffer. At point 2, the chamber was rinsed with buffer. Steps *i*, *ii*, and *iii* are discussed in the text.

mass load) while the dissipation increases (indicating increasing dissipative losses). After some time, the frequency starts to increase and the dissipation to decrease, in accord with previous reports (27–30). These two differentiated steps with respect to the changes in resonance frequency and dissipation correspond to the kinetics of two consecutive processes. Initially the vesicles adsorb intact to the empty crystal surface, producing high dissipative values due to the nonrigid character of the water-filled vesicles, and a marked frequency decrease due to the increase in total mass deposited over the surface (31). Later, when a critical threshold of coverage is reached, the vesicles undergo fusion (collapse) to form a stably supported bilayer, with no further uptake or release. The increase in frequency observed in this second step derives from the release of the water trapped inside the vesicles, meaning that there is a loss of surface-coupled mass. In this later step there is a decrease in dissipation, which reflects the transition from the soft dissipative vesicles to a more rigid and less dissipative flat bilayer.

Effect of SP-B on the fusion of zwitterionic LUVs

Fig. 1 *b* shows the profiles of a QCM experiment carried out with DOPC/SP-B LUVs. Upon the introduction into the QCM chamber of a suspension of DOPC LUVs containing 1% (w/w) SP-B (point 1), a rapid decrease in frequency is first observed (step *i*), indicating mass uptake with a maximum frequency shift of $\Delta f \sim -27.5$ Hz, accompanied by an increase of dissipation $\Delta D \sim 2.5 \times 10^{-6}$. These values are markedly different from those obtained with protein-free DOPC vesicles, where Δf is ~−60 Hz and $\Delta D \sim 9.5 \times 10^{-6}$ (three times larger changes than in the presence of SP-B). After this initial change, there is a transient decrease in dissipation and a very small increase in frequency (step *ii*). After a few minutes, this development reverses and the frequency steadily decreases again (step *iii*), with a parallel increase in dissipation. This process is only halted when the chamber is rinsed with buffer (point 2). Thus, in contrast to protein-free vesicles, the SP-B vesicles do not bind to the same extent as intact vesicles on the silica surface before they collapse, nor do they form the same stable supported bilayer with low dissipation and a frequency change of ~−26 Hz. The profiles from the different overtones overlap substantially in the early stages of the vesicle adsorption step, but start to deviate in the subsequent steps. This is a clear indication of deviation from simple Sauerbrey conditions, i.e., there is formation of soft surface layers whose oscillations are not rigidly coupled to the crystal oscillations. The penetration depth of the oscillations into the liquid differs depending on the overtone (in the range of 70–150 nm), and the differences between their normalized frequencies reflect the thickness of the surface layer. In subsequent *f-D* time profiles (which generally show overtone deviations to the same extent as those in Fig. 1 *b*), for clarity we will show only overtone 7.

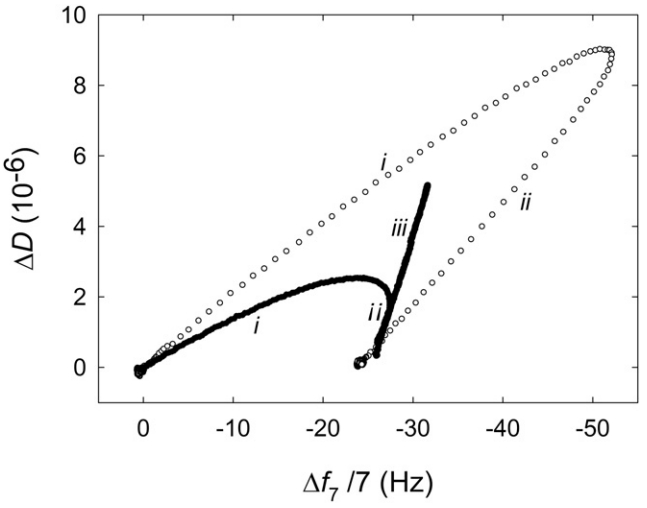

FIGURE 2 Dissipation/frequency shift correlation for the collapse of DOPC or DOPC/SP-B vesicles on a silica surface. Changes in dissipation are plotted against the frequency shift as recorded from the seventh overtone (Fig. 1) upon adsorption and collapse of DOPC vesicles (0.1 mg/mL) on a silica surface, in the absence (*open circles*) or presence (*solid circles*) of 1% SP-B (w/w).

The dissipation profile associated with adsorption and collapse of DOPC/SP-B vesicles is also remarkably different from that obtained from pure lipid vesicles. The collapse of protein-containing vesicles leads to only a transient decrease in dissipation after the initial increase. Once a minimum in dissipation is reached, the *D*-values increase again, more steeply (relative to changes in *f*) than observed in the initial increase associated with adsorption of the first vesicles. This suggests that the collapse in the presence of SP-B continues with a substantial reorganization of the lipid layer and ends in a highly dissipative structure. This may be illustrated more clearly by a plot of ΔD versus Δf for both pure DOPC and DOPC/SP-B samples (Fig. 2). Such a plot allows us to distinguish the two phases leading to vesicle collapse. In the first step (step *i*), which presumably leads to the saturation of the quartz crystal with adsorbed vesicles, there is a progressive increase in dissipation accompanying the decay in resonation frequency. The frequency increase associated with fusion of the vesicles at the crystal surface in step *ii* is clearly accompanied by a decrease in the dissipation factor. Superimposing the $\Delta D/\Delta f$ plot (Fig. 2) for the samples containing SP-B gives a clearer idea of their different behavior compared with pure lipid vesicles.

Several quantitative differences are observed. The initial gradient of the plot is substantially lower for the SP-B containing vesicles, and then the decrease in dissipation factor sets in at a Δf of 25 Hz (rather than the 50 Hz seen for protein-free vesicles). The initial gradient corresponds to conditions well below any critical coverage and represents intact vesicles adsorbing at the silica interfaces. The lower dissipation value per frequency implies that the SP-B containing vesicles have a lower dissipative conformation

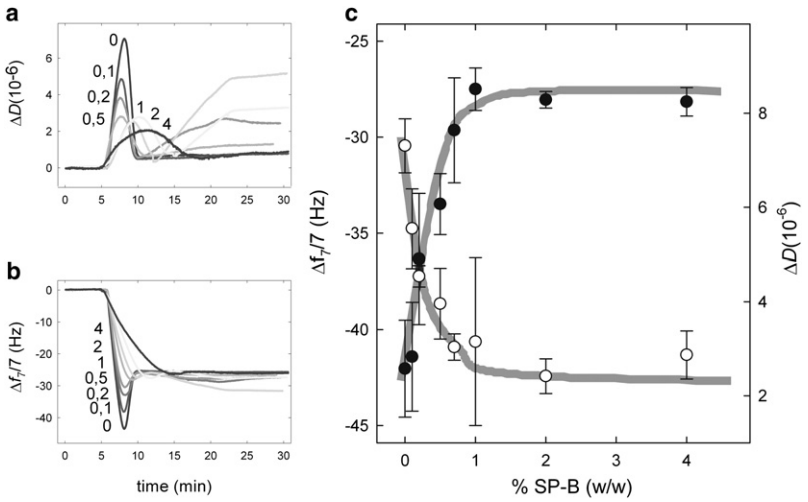

FIGURE 3 Effect of protein density on the SP-B-promoted adsorption and collapse of DOPC vesicles on a silica surface. Changes in dissipation (*a*) and frequency (*b*) are compared during adsorption and collapse of 0.1 mg/mL DOPC vesicles containing different proportions of SP-B. Each curve corresponds to a different proportion of SP-B, with the different gray tones indicating increasing proportions of SP-B. (*c*) Titration of maximum dissipation values (*open circles*) and minimum frequency shift (*closed symbols*) versus the SP-B proportion in DOPC bilayers. Bars correspond to absolute error after averaging three different samples of each protein concentration. Lines are intended to guide the eye.

compared to protein-free vesicles. The lower frequency shift seen at the critical coverage could imply that fewer vesicles are present. However, the time at which the critical coverage is reached, although earlier for these SP-B-containing vesicles, is not sufficiently earlier to suggest that substantially fewer vesicles have arrived at the surface to explain the 50% lower frequency shift. An alternative explanation is that the conformation of the SP-B containing vesicles is compressed on the surface, resulting in both a lower dissipation and lower frequency per vesicle and potentially a larger surface coverage. The lower frequency implies that less water is coupled at the surface per vesicle, implying that water leaks out of the vesicles. The step that is unique for SP-B-containing membranes (step *iii*) is seen as a steep rise in Fig. 2, and is likely related to SP-B-promoted further association of additional lipid/protein material to the supported layer.

To obtain more insight into the amount of SP-B needed to elicit these changes, we recorded the dissipation (Fig. 3 *a*) and frequency (Fig. 3 *b*) changes of overtone 7 for samples containing different proportions (0–4% w/w) of SP-B. As the proportion of SP-B in the membranes increases, Δf_{min} becomes less negative and ΔD_{max} decreases, which indicates that in the presence of SP-B less material is present on the surface at the critical threshold of coverage at which vesicle rupture is initiated. The presence of SP-B appears to promote vesicle conformational changes, fusion, and membrane reorganization. Although vesicles with low SP-B concentrations reach critical coverage somewhat earlier than protein-free vesicles, above a threshold concentration of ~0.7% SP-B, the rupture of vesicles shifts to longer times. This is accompanied by broadened dissipation peaks (Fig. 3 *a*). At first sight, this appears to contradict the suggestion that SP-B enhances collapse. A possible explanation is that above certain protein densities, the net positive charge of SP-B (~+7 at pH 7) could introduce repulsive contributions that obstruct membrane association. The maximum achieved values for dissipation and minimum values for frequency shifts versus SP-B concentration are reached from ~1% protein (Fig. 3 *c*). Of interest, this is close to the physiological proportions of the protein in native LS membranes.

Note that in the second part of the dissipation profiles for SP-B/DOPC vesicles, where a further increase in dissipation is observed as promoted by SP-B once the vesicles have collapsed (Fig. 3 *a*), there is no simple dependence of SP-B concentration. Our interpretation is that the increase in protein proportion could produce overlapping effects, including protein-promoted membrane lysis of some of the attached membranes and association of membrane patches from the vesicles in the bulk phase, yielding a complex pattern that is difficult to interpret.

We carried out analogous studies of the collapse of DOPC vesicles with and without the bacterial cationic lipopeptide PMB (see the Supporting Material for more information). Of interest, we see the same ΔD_{max} with 2% polymyxin as for SP-B (see Fig. S1 in the Supporting Material), indicating that PMB also facilitates collapse and promotes water leakage from vesicles once they have covered the surface of the QCM crystal to a similar extent. However, polymyxin never showed the last step of a steady increase of dissipation/decrease of frequency that is characteristic of membrane reorganization in the presence of SP-B.

Effect of SP-B on the fusion of anionic unilamellar vesicles

It has been reported that SP-B interacts selectively with negatively charged phospholipids, particularly with the phosphatidylglycerol fraction of surfactant (32,33). To analyze the possible effects of the presence of negatively charged lipids on the ability of SP-B to promote collapse of membranes, we monitored the collapse of DOPC/POPG (8:2, w/w) unilamellar vesicles in the presence of SP-B (Fig. 4). For all experiments with anionic vesicles, we included 2 mM $CaCl_2$ to reduce the repulsion effect between negatively charged vesicles and facilitate the collapse. In the absence of SP-B, these mixed vesicles show the same

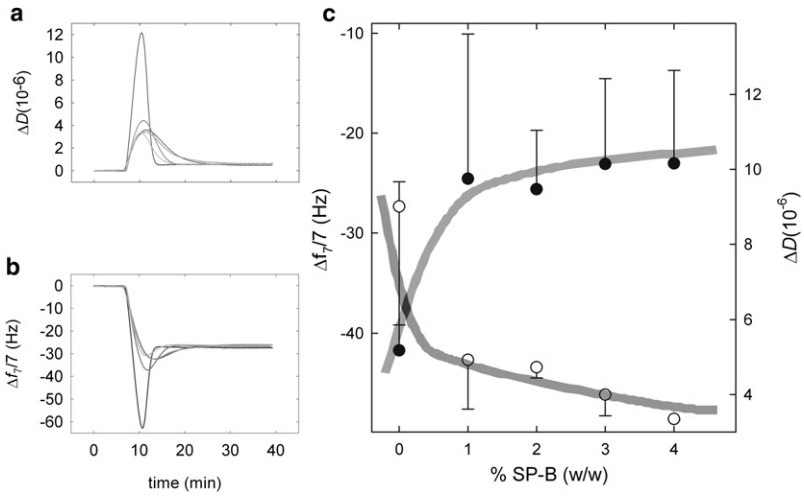

FIGURE 4 Effect of protein density on the SP-B-promoted adsorption and collapse of DOPC/DOPG vesicles on a silica surface. Changes in dissipation (*a*) and frequency (*b*) are compared during adsorption and collapse of 0.1 mg/mL DOPC/DOPG (8:2, w/w) vesicles containing different proportions of SP-B. Each curve corresponds to a different proportion of SP-B as in Fig. 3. (*c*) Titration of maximum dissipation values (*open circles*) and minimum frequency shift (*closed circles*) versus the SP-B proportion in DOPC/DOPG bilayers. Bars correspond to absolute error after averaging three different samples of each protein concentration, with only half the error plotted for the sake of clarity. Lines are intended to guide the eye.

two-step bind-and-collapse signature as pure DOPC vesicles. This agrees with observations by Morigaki and Tawa (34) based on surface plasmon resonance and surface plasmon fluorescence spectroscopy. These authors noted that essentially all lipid mixtures show the same type of autocatalytic transformation into planar bilayers, although the degree of lipid charge affects the critical vesicle concentration where this occurs.

The presence of SP-B in DOPC/POPG membranes decreases the dissipation maximum (Fig. 4 *a*) and makes the frequency minimum that precedes the collapse of vesicles less negative (Fig. 4 *b*), as occurs in zwitterionic membranes. However, in contrast to the effect of SP-B in DOPC vesicles, the presence of SP-B in DOPC/POPG membranes does not produce increasing dissipative values once the vesicles collapse, indicating that collapse of anionic membranes ends in a stable bilayer without further material adhesion or release, irrespective of the presence of SP-B. Nevertheless, SP-B also promotes rupture and reorganization of membranes in the presence of anionic lipids. Fig. 4 *c* plots the minimum shift values for frequency and maximum in dissipation for DOPC/POPG vesicles versus the proportion of SP-B in the membranes. Again, a close to maximum effect of SP-B seems to be reached from 1% protein by weight, which corresponds to the physiological proportions of SP-B in surfactant membranes. The kinetics of the collapse of anionic membranes in the presence of SP-B seems to show a delay similar to that observed in zwitterionic membranes when the proportion of the protein increased above 0.5%.

SP-B effect in surfactant-like lipid membrane reorganization

For simplicity and practicality, the experiments described so far were all conducted in DOPC or DOPC/DOPG membranes, which remain in the liquid disordered state at ambient temperatures. To obtain data under conditions closer to the in vivo situation, we also carried out experiments with bilayers containing DPPC, the most abundant phospholipid species in LS membranes. We assessed vesicles made of two different lipid mixtures—DPPC/POPC (7:3, w/w) and DPPC/POPC/POPG (50:25:25, w/w/w)—to a final lipid concentration of 0.1 mg/mL in the presence or absence of SP-B at 2% (w/w) protein/lipid ratio. The QCM-D time-dependent profiles shown in Fig. 5 were obtained at 40°C to ensure that the membranes were entirely in a fluid state, which we observed to be strictly required for promoting a rapid vesicle collapse. Experiments carried out at lower temperatures (data not shown) showed no collapse of vesicles with this composition, suggesting that a proper membrane dynamics is also important to facilitate rapid reorganization of membranes upon collapse at the surface of the quartz crystal, and emphasizing the usefulness of working with lipids that remain liquid-disordered under all practical conditions. The different lipid composition induced some differences in the collapse of lipid-protein vesicles. The membranes made of the mixture DPPC/POPC behaved similarly to the DOPC and DOPC/DOPG vesicles. Thus the presence of SP-B (Fig. 5 *b*) in the vesicles showed a decreased peak in dissipation and reduced frequency shift before collapse compared to that observed in the absence of protein (Fig. 5 *a*). The vesicles made of DPPC/POPC/POPG showed a relatively small dissipation peak even in the absence of protein (Fig. 5 *c*), probably reflecting an intrinsic, particularly dynamic character of these membranes, which makes them collapse more readily on the silica surface. The presence of SP-B promoted the collapse of this ternary lipid mixture even further, with the dip in frequency disappearing and only a small peak in dissipation observed. The frequency profile suggests that SP-B promotes a practically direct conversion of lipid vesicles into a single supported bilayer (Fig. 5 *d*), almost bypassing the transient surface-attached vesicle stage. However, the dissipation profiles obtained with this lipid mixture are rather unstable and noisy, probably as a consequence of complex lipid reorganizations.

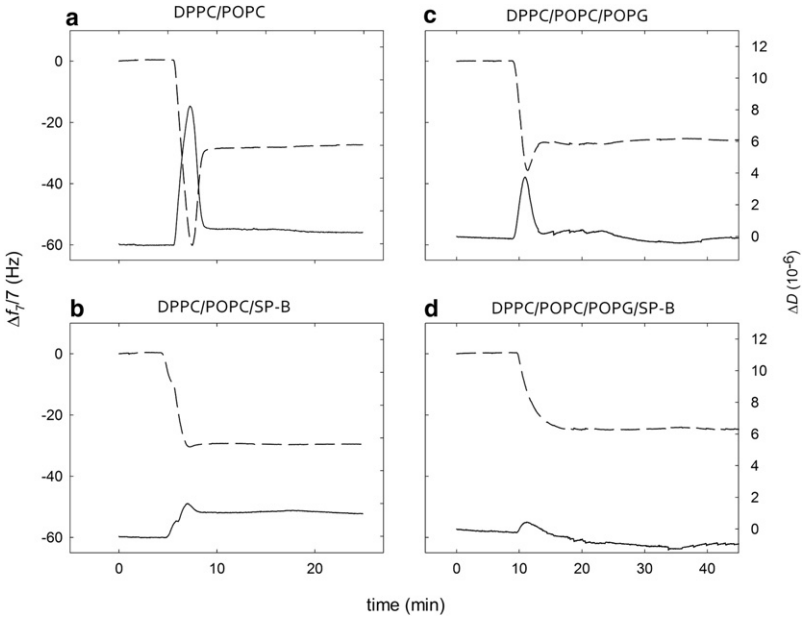

FIGURE 5 Effect of SP-B on the adsorption and collapse of DPPC/POPC or DPPC/POPC/POPG vesicles on a silica surface. The QCM-D profiles of frequency shift (*dashed line*) and dissipation changes (*solid line*) of the seventh overtone are plotted during adsorption and collapse of LUVs made of DPPC/POPC (7:3, w/w) (*a* and *b*) or DPPC/POPC/POPG (50/25/25, w/w/w) (*c* and *d*), in the absence (*a* and *c*) or presence (*b* and *d*) of 2% SP-B (w/w). The silica crystals were preequilibrated in HEPES 50 mM, pH 7, NaCl 150 mM.

Incorporation of SP-B/lipid complexes into preformed bilayers

In addition to monitoring time-dependent vesicle collapse, QCM-D can be used to assess whether additional layers can be incorporated into supported bilayers once they have been formed on the surface of the crystal. This is particularly relevant in view of the potential role of SP-B in the biogenesis of LS structures such as multivesicular bodies, lamellar bodies, and tubular myelin. We therefore undertook to explore the potential of SP-B to promote membrane-membrane contacts. The experimental design was as follows (Fig. 6 *a*): After the initial collapse of the SP-B/DOPC vesicles led to a stable value of dissipation and frequency (corresponding to time point *iii* in Fig. 1 *b*), the surface was rinsed with buffer (point 2). After a stable baseline was obtained, the supported lipid/protein film was exposed to a second batch of SP-B/DOPC vesicles with the same composition (point 3), which led to a further continuous increase in dissipation and a lower frequency value that was halted only when the chamber was rinsed again with buffer (point 4). We interpret this to mean that exposure to a second batch of vesicles induces the deposition of more material over the stable preformed bilayer. We carried out control experiments in which DOPC vesicles without SP-B were added on top of a supported membrane that was preformed on the QCM surface from SP-B/DOPC vesicles (Fig. 6 *b*), or DOPC vesicles with

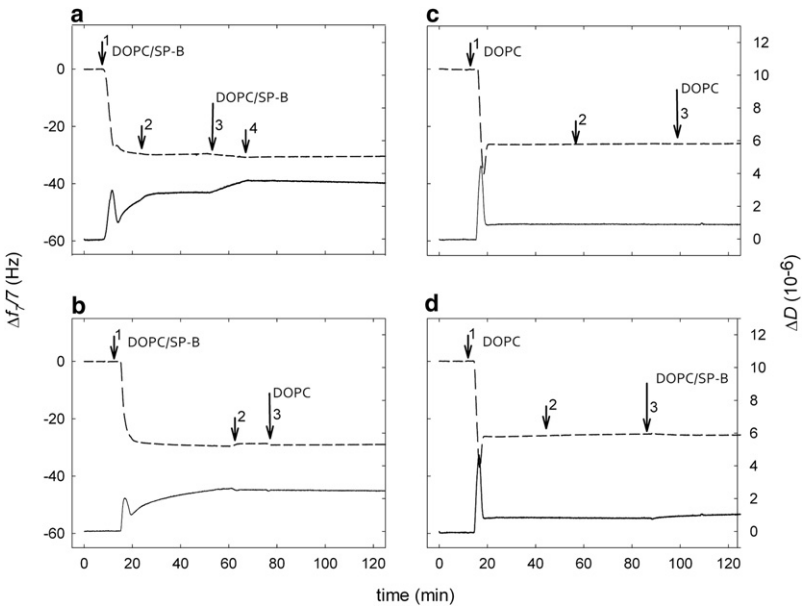

FIGURE 6 Ability of SP-B to promote incorporation of phospholipids into a preformed supported DOPC bilayer. Changes in frequency, Δf (*dashed line*), and dissipation, ΔD (*solid line*), as a function of time were monitored in QCM-D experiments where the formation of a supported lipid or lipid/protein layer was followed by exposure of the supported membrane to a second batch of lipid or lipid/protein vesicles. In point 1, 0.1 mg/mL of DOPC vesicles in the presence (*a* and *b*) or absence (*c* and *d*) of 2% SP-B (w/w) were introduced into the QCM-D chamber. In point 2, the chamber was rinsed with buffer until a stable baseline was obtained. In point 3, the silica crystal bearing the supported lipid or lipid/protein layer was exposed to a second batch of 0.1 mg/mL DOPC vesicles with (*a* and *d*) or without (*b* and *c*) 2% SP-B. In panel *a*, the steady increase in dissipation and decrease in frequency initiated upon introduction of the second batch of DOPC/SP-B vesicles stopped only after the QCM-D chamber was rinsed again with buffer (point 4).

SP-B were added over a preformed bilayer without SP-B (Fig. 6 *d*). These experiments show no additional association with the supported layer if no SP-B is included in both the bulk vesicles and the supported membrane, suggesting that either a dynamic role of SP-B is required, which cannot be properly achieved when SP-B is present only in the immobilized membrane, or SP-B-promoted protein-protein interactions are required to facilitate membrane-membrane apposition.

A similar experiment carried out with DOPC/POPG (8:2) vesicles shows a qualitatively similar behavior (Fig. S2). Again, SP-B is required in both the supported membrane and the bulk vesicles to promote further incorporation of lipid into the supported layers.

Finally, we analyzed the interaction between differently charged lipids. In one experiment, DOPC/SP-B bulk vesicles were added to a supported layer that had been preformed by anionic DOPC/POPG/SP-B complexes (Fig. S3 *a*), and the sequence was reversed in another experiment (Fig. S3 *b*). Of interest, no significant changes in frequency or dissipation were detected when membranes of different compositions were confronted. This result suggests that the presence of SP-B in the two membrane sides is not the only requisite; the two membranes have to present an appropriate state of charge and/or a competent protein conformation, which was previously shown to be critically influenced by the presence of negatively charged lipid species (33).

DISCUSSION

Supported lipid bilayers have been popular as model systems of cell membranes (35–38). The creation of supported lipid bilayers by the spreading of lipid vesicles on hydrophilic supports is attractive because of its simplicity and reproducibility, but the driving forces involved in the adsorption of vesicles and supported planar bilayer formation are still poorly understood. In this work, the formation of supported planar bilayers was analyzed with the use of QCM-D. Previous results from QCM-D established that vesicles made of PC lipids in fluid phase form support lipid bilayers on the silica surface (29,39). Building on these observations, we increased the complexity of the lipid system by including SP-B protein (the most important surfactant protein for respiratory function) with different vesicles. Despite this complexity, we were able to observe reproducible effects of SP-B on vesicle adsorption and bilayer formation.

The QCM profiles of the vesicles with and without SP-B show that SP-B strongly affects the collapse of DOPC vesicles. The experiments suggest that fusion and reorganization of vesicles are promoted by the presence of SP-B, leading to an early collapse with, in some cases, no apparent need for a threshold surface coverage. Clearly, the presence of SP-B significantly alters the conformation of surface-adsorbed vesicles before rupture. The vesicles adopt a lower dissipative state, and less water is coupled per vesicle. It is likely that SP-B allows the membrane-surface interactions to deform the vesicle shape to a greater degree. SP-B was previously shown to promote the leakage of aqueous solutes from phospholipid vesicles (5,18), and to induce formation of surface-attached membrane discs (40–42). Protein-promoted vesicle dehydration and membrane flattening at the silica surface could explain the differences in mass and dissipation profiles observed upon deposition of SP-B-containing vesicles. The perturbation of membrane structure induced by SP-B likely diminishes the activation barriers to collapse, and may reduce the critical surface colonization level required for vesicle rupture and fusion. This argues in favor of considering SP-B as a catalyzer that reduces the total activation energy required for the membrane collapse reaction to proceed. This activity observed under the particular in vitro conditions assayed here is consistent with the role proposed for SP-B in LS membranes (2,21), i.e., promoting reorganization of surfactant complexes at the interface and lipid exchange between surfactant storages and the interfacial surface-active film.

As previously reported in a study of lipid vesicle deposition over silica surfaces (43), there are many experimental parameters, such as buffer composition, pH, temperature, and vesicle concentration, that can influence the kinetics of supported bilayer formation. Two pathways of bilayer formation have been proposed, both of which are in agreement with the results presented here. The classical pathway, described by Keller and Kasemo (29), is based on an adsorption-rupture process that includes passage through a critical vesicle density on the surface. The second pathway, described by Dimitrievski et al. (44) and Richter et al. (45), is based on a direct rupture process that results from the surface contacts of each vesicle and is independent of the density of vesicles on the surface. The first mechanism seems to explain the collapse of our membrane vesicles in the absence of protein or in the presence of small proportions of SP-B (well below 1% w/w). However, when the proportion of SP-B is $\geq 1\%$, vesicle fusion is delayed and the change in dissipation and frequency is not so pronounced, supporting the idea that there is no need for the vesicles to cover all of the crystal before starting to break as they interact with the crystal surface, which agrees with the second model proposed. The fact that the maximum effect of SP-B in the reorganization of supported lipid layers is reached at protein densities in the order of the amounts of SP-B thought to exist in native pulmonary surfactant argues in favor of the physiological significance of the features observed in the QCM-D setup.

A unique feature of the surface colonization by SP-B/DOPC vesicles is the reproducibly high dissipation increase from time point *ii* to *iii* (Fig. 1 *b*), which is associated with a modest frequency change, leading to a very steep line in an *f-D* plot (Fig. 2). This last step has been interpreted in terms of SP-B favoring the adsorption of additional material and the reorganization of the adsorbed material into a much

more dissipative type of structure. SP-B interacts selectively with negatively charged phospholipids, particularly with the phosphatidylglycerol fraction of surfactant (33,46). We observe a distinct effect of including anionic lipids in our vesicles. As for zwitterionic vesicles, SP-B promotes the rupture and reorganization of membranes (Fig. 4), again reaching a plateau around 1% SP-B. However, in the presence of anionic phospholipids, the kinetics of the collapse is not so delayed, probably due to the presence of the negatively charged phospholipids, which can diminish the repulsive effect when a high concentration of SP-B is reached in the vesicles. Divalent ions such as Ca^{2+} are known to accelerate the membrane fusion process by interacting with the phosphate groups of the lipids and the negatively charged silica surface (45). As a consequence, the adhesion strength between the lipids and the support increases, producing more stable layers with stable dissipative values at the end of the experiment (as shown in Fig. 4 *b*).

Some models suggest that SP-B could be particularly important for ensuring an efficient flow of lipid molecules between different surfactant structures and with multilayer surface-associated films. The presence of SP-B in films subjected to compression results in associated bilayer patches that can be reinserted into the air-liquid interface upon expansion (40). Our QCM-D approach was particularly useful for assessing whether SP-B promotes the association of membrane vesicles onto a preformed supported bilayer. This is indeed the case (Fig. 6 *a*) provided that 1), there is SP-B in both membrane sides; and 2), the two membranes have a similar lipid composition in terms of charge. It has to be mentioned that the increase in dissipation seems to be much more sensitive to further adsorption of several lipid layers than the frequency shift, suggesting either that changes in frequency are less sensitive to deposition of membrane layers progressively separated from the surface of the crystal, or that deposition of additional membranes is accompanied by an SP-B-promoted reorganization to a more dissipative type of structure.

The QCM-D approach provides additional information to interpret the role of SP-B in remodeling surfactant membrane complexes, which was previously analyzed in classical approaches by studying model liposomes in the absence or presence of the protein. Analyses by electron microscopy of the effect of SP-B on the structure of liposome preparations (47) or the effect of the protein on the fluorescence of liposomes labeled with proper fluorescent probes (5,17) revealed the ability of SP-B to promote membrane-membrane contacts and to facilitate the exchange of phospholipids molecules between contacting membranes. However, experiments carried out using this classical ''bulk phase'' approach provide averaged behaviors and can hardly permit a detailed analysis of the vectorial requirements for SP-B-promoted membrane-membrane interactions, which can be assessed at the surface of the quartz crystal in the QCM, in the absence of spurious probes. An important advantage of the QCM-D technique is that it allows one to dissect the effect of parameters such as the lipid or protein composition in the two sides of the associating membranes. Our results suggest that SP-B-promoted formation of multilayer membrane arrays requires the presence of the protein in both sides of the membrane, in a somehow compatible state. We speculate that close association and packing of surfactant membranes may require the occurrence of SP-B/SP-B interactions, perhaps implying a competent conformation of the two interacting entities defined by the proper lipid composition, especially with regard to the presence or absence of anionic lipids. It was previously shown that the conformation of SP-B is critically influenced by the presence of negatively charged lipid species (33). In this sense, QCM-D provides a novel and valuable tool to explore determinants of membrane reorganization and packing as promoted by SP-B, a basic process that likely is essential for the biogenesis of lamellar bodies and their unpacking upon secretion to form tubular myelin, and the establishment of multilayered surface films competent to stabilize the respiratory surface against the demanding physical conditions of breathing mechanics.

SUPPORTING MATERIAL

Three figures and a comparison with the effects of the surfactant-mimetic polymyxin B are available at http://www.biophysj.org/biophysj/supplemental/S0006-3495(09)01016-9.

This work was inspired by preliminary studies carried out by K. H. Kristoffersen. We thank Drs. T. Thormann, C. Johansen, and P. Sørensen for stimulating discussions.

This research was supported by grants from the Spanish Ministry of Science (BIO2006-03130, CONSOLIDER-INGENIO 2010 CSD2007-00010), Community of Madrid (S0505/MAT/0283), Complutense University, and Marie Curie Networks (CT-04-007931 and CT-04-512229 to E.J.C. and J.P.-G.).

REFERENCES

1. Zuo, Y. Y., R. A. Veldhuizen, A. W. Neumann, N. O. Petersen, and F. Possmayer. 2008. Current perspectives in pulmonary surfactant–inhibition, enhancement and evaluation. *Biochim. Biophys. Acta.* 1778:1947–1977.
2. Perez-Gil, J. 2008. Structure of pulmonary surfactant membranes and films: the role of proteins and lipid-protein interactions. *Biochim. Biophys. Acta.* 1778:1676–1695.
3. Perez-Gil, J., and K. M. Keough. 1998. Interfacial properties of surfactant proteins. *Biochim. Biophys. Acta.* 1408:203–217.
4. Blanco, O., and J. Perez-Gil. 2007. Biochemical and pharmacological differences between preparations of exogenous natural surfactant used to treat respiratory distress syndrome: role of the different components in an efficient pulmonary surfactant. *Eur. J. Pharmacol.* 568:1–15.
5. Hawgood, S., M. Derrick, and F. Poulain. 1998. Structure and properties of surfactant protein B. *Biochim. Biophys. Acta.* 1408:150–160.
6. Clark, J. C., S. E. Wert, C. J. Bachurski, M. T. Stahlman, B. R. Stripp, et al. 1995. Targeted disruption of the surfactant protein B gene disrupts surfactant homeostasis, causing respiratory failure in newborn mice. *Proc. Natl. Acad. Sci. USA.* 92:7794–7798.
7. Ikegami, M., J. A. Whitsett, P. C. Martis, and T. E. Weaver. 2005. Reversibility of lung inflammation caused by SP-B deficiency. *Am. J. Physiol. Lung Cell. Mol. Physiol.* 289:L962–L970.

8. Nogee, L. M. 2004. Alterations in SP-B and SP-C expression in neonatal lung disease. *Annu. Rev. Physiol.* 66:601–623.
9. Vorbroker, D. K., S. A. Profitt, L. M. Nogee, and J. A. Whitsett. 1995. Aberrant processing of surfactant protein C in hereditary SP-B deficiency. *Am. J. Physiol.* 268:L647–L656.
10. Weaver, T. E., and J. J. Conkright. 2001. Function of surfactant proteins B and C. *Annu. Rev. Physiol.* 63:555–578.
11. Foster, C. D., P. X. Zhang, L. W. Gonzales, and S. H. Guttentag. 2003. In vitro surfactant protein B deficiency inhibits lamellar body formation. *Am. J. Respir. Cell Mol. Biol.* 29:259–266.
12. Stahlman, M. T., M. P. Gray, M. W. Falconieri, J. A. Whitsett, and T. E. Weaver. 2000. Lamellar body formation in normal and surfactant protein B-deficient fetal mice. *Lab. Invest.* 80:395–403.
13. Morrow, M. R., J. Perez-Gil, G. Simatos, C. Boland, J. Stewart, et al. 1993. Pulmonary surfactant-associated protein SP-B has little effect on acyl chains in dipalmitoylphosphatidylcholine dispersions. *Biochemistry.* 32:4397–4402.
14. Vandenbussche, G., A. Clercx, M. Clercx, T. Curstedt, J. Johansson, et al. 1992. Secondary structure and orientation of the surfactant protein SP-B in a lipid environment. A Fourier transform infrared spectroscopy study. *Biochemistry.* 31:9169–9176.
15. Cruz, A., C. Casals, I. Plasencia, D. Marsh, and J. Pérez-Gil. 1998. Depth profiles of pulmonary surfactant protein B in phosphatidylcholine bilayers, studied by fluorescence and electron spin resonance spectroscopy. *Biochemistry.* 37:9488–9496.
16. Poulain, F. R., L. Allen, M. C. Williams, R. L. Hamilton, and S. Hawgood. 1992. Effect of surfactants apolipoproteins on liposome structure: implications for tubular myelin formation. *Am. J. Physiol.* 262:L730–L739.
17. Oosterlaken-Dijksterhuis, M. A., M. van Eijk, L. M. van Golde, and H. P. Haagsman. 1992. Lipid mixing is mediated by the hydrophobic surfactant protein SP-B but not by SP-C. *Biochim. Biophys. Acta.* 1110:45–50.
18. Ryan, M. A., X. Qi, A. G. Serrano, M. Ikegami, J. Perez-Gil, et al. 2005. Mapping and analysis of the lytic and fusogenic domains of surfactant protein B. *Biochemistry.* 44:861–872.
19. Schram, V., and S. B. Hall. 2001. Thermodynamic effects of the hydrophobic surfactant proteins on the early adsorption of pulmonary surfactant. *Biophys. J.* 81:1536–1546.
20. Serrano, A. G., M. Ryan, T. E. Weaver, and J. Perez-Gil. 2006. Critical structure-function determinants within the N-terminal region of pulmonary surfactant protein SP-B. *Biophys. J.* 90:238–249.
21. Serrano, A. G., and J. Perez-Gil. 2006. Protein-lipid interactions and surface activity in the pulmonary surfactant system. *Chem. Phys. Lipids.* 141:105–118.
22. Rodahl, M., F. Höök, C. Fredriksson, C. A. Keller, A. Krozer, et al. 1997. Simultaneous frequency and dissipation factor QCM measurements of biomolecular adsorption and cell adhesion. *Faraday Discuss.* 107:229–246.
23. Bingen, P., G. Wang, N. F. Steinmetz, M. Rodahl, and R. P. Richter. 2008. Solvation effects in the quartz crystal microbalance with dissipation monitoring response to biomolecular adsorption. A phenomenological approach. *Anal. Chem.* 80:8880–8890.
24. Voinova, M. V., M. Rodahl, M. Jonson, and B. Kasemo. 1999. Viscoelastic acoustic response of layered polymer films at fluid-solid interfaces: continuum mechanics approach. *Phys. Scr.* 59:391–396.
25. Perez-Gil, J., A. Cruz, and C. Casals. 1993. Solubility of hydrophobic surfactant proteins in organic solvent/water mixtures. Structural studies on SP-B and SP-C in aqueous organic solvents and lipids. *Biochim. Biophys. Acta.* 1168:261–270.
26. Hook, F., M. Rodahl, B. Kasemo, and P. Brzezinski. 1998. Structural changes in hemoglobin during adsorption to solid surfaces: effects of pH, ionic strength, and ligand binding. *Proc. Natl. Acad. Sci. USA.* 95:12271–12276.
27. Keller, C. A., K. Glasmästar, V. P. Zhdanov, and B. Kasemo. 2000. Formation of supported membranes from vesicles. *Phys. Rev. Lett.* 84:5443–5446.
28. Reimhult, E., F. Hook, and B. Kasemo. 2003. Intact vesicle adsorption and supported biomembrane formation from vesicles in solution: influence of surface chemistry, vesicle size, temperature, and osmotic pressure. *Langmuir.* 19:1681–1691.
29. Keller, C. A., and B. Kasemo. 1998. Surface specific kinetics of lipid vesicle adsorption measured with a quartz crystal microbalance. *Biophys. J.* 75:1397–1402.
30. Justesen, P. H., T. Kristensen, T. Ebdrup, and D. E. Otzen. 2004. Investigating phospholipase action on vesicles and supported planar bilayers using a quartz crystal microbalance. *J. Coll. Int. Sci.* 279:399–409.
31. Yokoyama, N., M. Hirata, K. Ohtsuka, Y. Nishiyama, K. Fujii, et al. 2000. Co-expression of human chaperone Hsp70 and Hsdj or Hsp40 co-factor increases solubility of overexpressed target proteins in insect cells. *Biochim. Biophys. Acta.* 1493:119–124.
32. Reference deleted in proof.
33. Cruz, A., D. Marsh, and J. Perez-Gil. 1998. Rotational dynamics of spin-labelled surfactant-associated proteins SP-B and SP-C in dipalmitoylphosphatidylcholine and dipalmitoylphosphatidylglycerol bilayers. *Biochim. Biophys. Acta.* 1415:125–134.
34. Morigaki, K., and K. Tawa. 2006. Vesicle fusion studied by surface plasmon resonance and surface plasmon fluorescence spectroscopy. *Biophys. J.* 91:1380–1387.
35. Watts, T. H., A. A. Brian, J. W. Kappler, P. Marrack, and H. M. McConnell. 1984. Antigen presentation by supported planar membranes containing affinity-purified I-Ad. *Proc. Natl. Acad. Sci. USA.* 81:7564–7568.
36. Watts, T. H., H. E. Gaub, and H. M. McConnell. 1986. T-cell-mediated association of peptide antigen and major histocompatibility complex protein detected by energy transfer in an evanescent wave-field. *Nature.* 320:179–181.
37. Sackmann, E. 1996. Supported membranes: scientific and practical applications. *Science.* 271:43–48.
38. Salafsky, J., J. T. Groves, and S. G. Boxer. 1996. Architecture and function of membrane proteins in planar supported bilayers: a study with photosynthetic reaction centers. *Biochemistry.* 35:14773–14781.
39. Reimhult, E., F. Höök, and B. Kasemo. 2002. Vesicles adsorption on SiO_2 an TiO_2: dependence on vesicles size. *J. Chem. Phys.* 117:7401–7404.
40. Krol, S., M. Ross, M. Sieber, S. Kunneke, H. J. Galla, et al. 2000. Formation of three-dimensional protein-lipid aggregates in monolayer films induced by surfactant protein B. *Biophys. J.* 79:904–918.
41. Poulain, F. R., J. Akiyama, L. Allen, C. Brown, R. Chang, et al. 1999. Ultrastructure of phospholipid mixtures reconstituted with surfactant proteins B and D. *Am. J. Respir. Cell Mol. Biol.* 20:1049–1058.
42. Poulain, F. R., L. Allen, M. C. Williams, R. L. Hamilton, and S. Hawgood. 1992. Effects of surfactant apolipoproteins on liposome structure: implications for tubular myelin formation. *Am. J. Physiol.* 262:L730–L739.
43. Seantier, B., C. Breffa, O. Felix, and G. Decher. 2005. Dissipation-enhanced quartz crystal microbalance studies on the experimental parameters controlling the formation of supported lipid bilayers. *J. Phys. Chem. B.* 109:21755–21765.
44. Dimitrievski, K., E. Reimhult, B. Kasemo, and V. P. Zhdanov. 2004. Simulations of temperature dependence of the formation of a supported lipid bilayer via vesicle adsorption. *Colloids Surf. B Biointerfaces.* 39:77–86.
45. Richter, R., A. Mukhopadhyay, and A. Brisson. 2003. Pathways of lipid vesicle deposition on solid surfaces: a combined QCM-D and AFM study. *Biophys. J.* 85:3035–3047.
46. Pérez-Gil, J., C. Casals, and D. Marsh. 1995. Interactions of hydrophobic lung surfactant proteins SP-B and SP-C with dipalmitoylphosphatidylcholine and dipalmitoylphosphatidylglycerol bilayers studied by electron spin resonance spectroscopy. *Biochemistry.* 34:3964–3971.
47. Cruz, A., C. Casals, K. M. Keough, and J. Perez-Gil. 1997. Different modes of interaction of pulmonary surfactant protein SP-B in phosphatidylcholine bilayers. *Biochem. J.* 327:133–138.